Patterns of ^{18}F-FDG Uptake in Adipose Tissue and Muscle: A Potential Source of False-Positives for PET

Henry W.D. Yeung, MD[1]; Ravinder K. Grewal, MD[1]; Mithat Gonen, PhD[2]; Heiko Schöder, MD[1]; and Steven M. Larson, MD[1]

[1]Nuclear Medicine Service, Department of Radiology, Memorial Sloan-Kettering Cancer Center, New York, New York; and [2]Department of Epidemiology and Biostatistics, Memorial Sloan-Kettering Cancer Center, New York, New York

The routine use of PET/CT fusion imaging in a large oncology practice has led to the realization that ^{18}F-FDG uptake into normal fat and muscle can be a common source of potentially misleading false-positive PET imaging in the neck, thorax, and abdomen. The goal of this study was to characterize this normal variant of ^{18}F-FDG uptake in terms of incidence and characteristic extent. **Methods:** All body scans done on our PET/CT scanners in July and August 2002 were retrospectively reviewed. All cases in which increased ^{18}F-FDG uptake in the neck was not localized to lymph nodes or other obvious anatomic sites on the CT scans were included in this study. Sites of any unexplained ^{18}F-FDG uptake in the rest of the body were also recorded. **Results:** A total of 863 PET scans (476 males, 387 females; age, 2–88 y; mean age, 57 y) were reviewed. The following distinctive patterns of nonpathologic ^{18}F-FDG activity were observed: (a) neck fat, 20 patients (2.3%); (b) paravertebral uptake, 12 patients (1.4%); (c) perinephric fat, 7 patients (0.8%); (d) mediastinal fat, 8 patients (0.9%); (e) normal musculature, 12 patients (1.4%). Patients showing paravertebral uptake, perinephric fat, and mediastinal fat were all associated with the neck fat pattern, singly or in combination. On the other hand, patients showing the normal musculature pattern did not show any of the other uptake. In this analysis, the incidence of ^{18}F-FDG uptake in sites other than the neck is restricted to the patient population with neck fat uptake and may be an underestimation of the true incidence. Neck fat is found predominantly in females, whereas normal musculature is usually seen in males ($P < 0.01$, Fisher exact test). Neck fat is also seen significantly more in the pediatric population ($4/26 = 15\%$) than in the adult population ($16/837 = 1.9\%$) ($P < 0.01$, Fisher exact test). **Conclusion:** Increased ^{18}F-FDG uptake is sometimes seen in individual muscles and in adipose tissue in the neck and shoulder region, axillae, mediastinum, and perinephric regions. There is also associated ^{18}F-FDG uptake in the intercostal spaces in the paravertebral regions. ^{18}F-FDG uptake in neck fat is more commonly seen in female patients and the pediatric population. The pattern of uptake as well as the age and sex distribution suggest that the ^{18}F-FDG in fat is in the brown adipose tissue. It is important to recognize this uptake pattern to avoid false interpretation of this benign normal variant as a malignant finding on ^{18}F-FDG PET scans.

Key Words: ^{18}F-FDG; uptake; fat; muscle

Since the middle of 1995, ^{18}F-FDG PET scanning of the body has been a clinical tool for the evaluation of various cancers. Starting in a few large cancer centers, PET is now available in many major hospitals as well as numerous radiologic imaging centers. Very early on, nuclear medicine physicians and radiologists have noticed curvilinear ^{18}F-FDG uptake in the neck and supraclavicular region that was not associated with any radiologic or clinically evident pathology (Fig. 1). Because of the curvilinear configuration and the observation that it resolved on repeated scanning after pretreatment with oral diazepam, a muscle relaxant, it was widely accepted to be muscle activity secondary to patient anxiety (*1,2*).

The PET/CT scanner, a machine that combines a full-ring detector PET scanner and a multidetector helical CT in a single gantry, has been commercially available since the middle of 2001. Using this machine, the PET scan can be acquired immediately after the CT scan, with the patient in exactly the same position. The CT dataset of the combined PET/CT is used for the attenuation correction of PET emission images, eliminating the need for transmission scans, resulting in a shortening of the scan time by 40%–50%. The PET and CT images can also be fused into a single image, providing superior anatomic localization of the PET abnormalities hitherto impossible with PET scans and CT scans obtained separately. This new technology has been shown to increase diagnostic accuracy and decrease equivocal findings of PET scans (*3–5*).

At our institution, we have been doing PET/CT scans since December 2001. Occasionally, we noticed patients

FIGURE 1. Coronal image shows curvilinear ^{18}F-FDG uptake in neck and supraclavicular regions bilaterally, extending to axillae, not associated with any radiologic or clinically evident pathology.

with nonpathologic curvilinear neck ^{18}F-FDG uptake. To our surprise, we found that this did not always map to the skeletal muscle but rather to the adipose tissue in the neck and shoulder region. We also noticed that sometimes there was abnormal ^{18}F-FDG activity in the adipose tissue in other parts of the body, specifically in the mediastinum and the perinephric regions. ^{18}F-FDG activity in adipose tissue in the neck and shoulders has been reported (6,7), but uptake in the adipose tissue in the chest and abdomen has not been described. We undertook this study to further characterize ^{18}F-FDG uptake in the neck and its association with unexplained ^{18}F-FDG uptake in other locations of the body.

MATERIALS AND METHODS

All body scans done on our PET/CT scanners in July and August 2002 were retrospectively reviewed.

Image Acquisition

The images were acquired on either the Biograph PET/CT scanner (Siemens Medical Systems, CTI) or the Discovery LS PET/CT scanner (General Electric Medical Systems).

The Biograph system integrates CPS PET (HR+) and Siemens Emotion CT technologies with the PET-Syngo computer software. Emotion is a dual-slice CT system that can acquire images with a slice thickness of 1.0–10.0 cm. The HR+ PET tomograph has no septa, so that it can only acquire 3-dimensional (3D) datasets, with transaxial resolution of 4.5 mm full width at half maximum at 1-cm off-axis and 5.4 mm at 10-cm off-axis. The acquired PET and CT image datasets are registered on a Syngo image display and processing platform and fused to form a single image that shows PET abnormalities on the CT images. Spiral CT scans from the neck to the pelvis were obtained using the following parameters: 130-kV peak; 80 mAs; scan width, 5 mm; and feed/rotation, 12 mm. Immediately on completion of the CT, PET scans of the same area were acquired for 4–5 min per bed position.

The Discovery LS PET/CT scanner consists of a composite gantry housing a LightSpeed 4-slice CT system and the Advance NXi PET scanner. The Lightspeed CT can acquire images with a slice thickness of 0.6–5.0 cm. The PET scanner has a retractable septa so that it can acquire 2-dimensional (2D) or 3D image datasets in PET mode. In the 2D mode, transverse spatial resolution is 4.9, 5.3, and 6.1 mm at 1, 10, and 20-cm off-axis, respectively. The acquired PET and CT image datasets are registered on an eNTEGRA image display and processing platform (General Electric Medical Systems) and fused to form a single image that shows PET abnormalities on the CT images. Spiral CT scans from the neck to the pelvis were obtained using the following parameters: 0.8 s per rotation; 140-kV peak; 80 mAs for adults (as low as 60 mAs for children); slice thickness, 5 mm; and 4.25-mm interval in high-speed mode. Immediately on completion of the CT, PET scans of the same area were acquired in the 2D mode, for 4–5 min per bed position.

All patients were scanned after fasting for at least 6 h, but hydration with water was allowed. The scans were obtained about 1 h after intravenous injection of 444 MBq ^{18}F-FDG for adults and normalized by weight for patients < 18 y old. Patients were encouraged to rest comfortably in a small quiet room during the waiting period after radiotracer injection.

Patient Selection and Image Analysis

The PET scans were analyzed first, followed by the CT scans and, finally, the PET/CT fused images. All cases in which focal ^{18}F-FDG activity in the neck clearly exceeded the surrounding background activity, and was not mapped to any lymph nodes, other pathology, or normal tissues with known ^{18}F-FDG uptake—that is, the larynx and salivary glands—were selected for this study.

In this group of patients, we looked for different patterns of increased ^{18}F-FDG activity in the neck as well as the chest and abdomen as follows, based on the PET/CT fused images:

- Neck fat: bilateral curvilinear ^{18}F-FDG activity, with or without focal nodular area, extending from the neck inferiorly to the shoulders and sometimes to the axillae mapped to the adipose tissue (Figs. 1 and 2).
- Paravertebral uptake: foci of ^{18}F-FDG activity along the thoracic spine bilaterally, mapped to the paravertebral intercostal space (Fig. 3).
- Perinephric fat: curvilinear or focal activity mapped to the perinephric adipose tissue around the upper pole of the kidneys (Fig. 4).
- Mediastinal fat: focal activity in the mediastinum, mapped to the adipose tissue among the large vessels (Fig. 5).
- Normal musculature: ^{18}F-FDG activity mapped to well-defined muscles (Fig. 6).

The maximum standardized uptake value (SUV_{max}) of a region of interest encompassing the ^{18}F-FDG activity was recorded. The body weight and body mass index (BMI: kg/m^2) of the patients and a control group, matched for age and sex, randomly selected from the PET database of the same time period, were also calculated.

Statistical Analysis

The prevalence of neck fat and normal musculature in males and females as well as in adult and pediatric patients was compared with the Fisher exact test. A control group was selected,
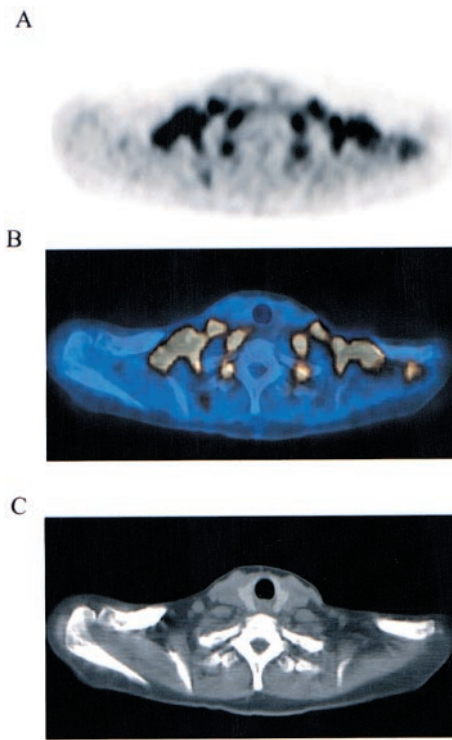
FIGURE 2. Transaxial slices of PET (A), CT (C), and fusion (B) images at supraclavicular level show ^{18}F-FDG activity mapped to adipose tissue.

matched by age and sex, from the patients who had PET scans in the same period but did not display ^{18}F-FDG uptake in fat. The weight and BMI of the patients with ^{18}F-FDG uptake were compared with those of the control group using a Wilcoxon test.

RESULTS

A total of 863 body scans were reviewed. The patient population comprised of 476 males and 387 females (mean age, 57 y; range, of 2–88 y). Thirty-two patients (3.7%) fulfilled the inclusion criteria of having ^{18}F-FDG activity in the neck not explained by normal structures or pathologies as seen on the concomitant CT scans. The mean dose of ^{18}F-FDG was 443 ± 26.7 MBq for adults, normalized by weight for patients < 18 y old. The average time interval between injection and the start of image acquisition was 69.6 ± 15.2 min. The PET/CT scans of these 32 patients were further reviewed, and the results are shown in Table 1. A summary of the findings is shown in Table 2.

Of the 32 scans, neck fat was seen on 20 scans (2.3% of total), whereas normal musculature was seen on 12 scans (1.4%). Paravertebral uptake, perinephric fat, and mediastinal fat were seen on a smaller number of scans and were all associated with neck fat—that is, seen in the same patient.

The SUV_{max} of all 5 patterns showed wide variation, ranging from 1.9 to 20. The average SUV_{max} of the 5 patterns were close to or >5, well into the commonly accepted pathologic range. Specifically, the average SUV_{max} of neck fat was 7.7 (range, 1.9–20). Cohade et al., in a
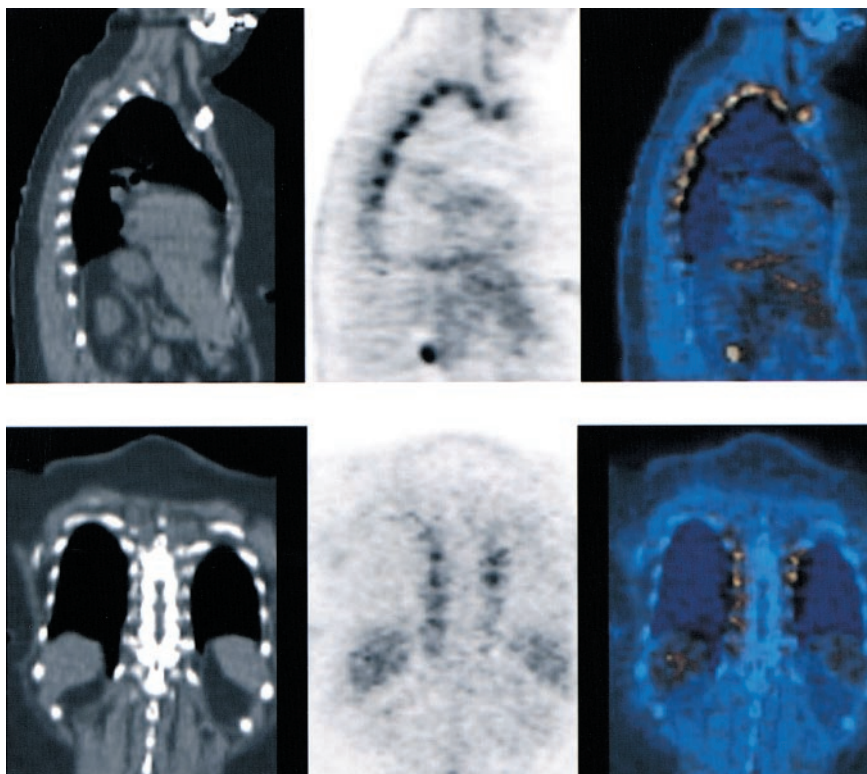
FIGURE 3. Foci of ^{18}F-FDG activity along thoracic spine bilaterally, mapped to paravertebral intercostal space. Sagittal slices (top) and coronal slices (bottom), with CT on left, PET in middle, and fusion images on right.
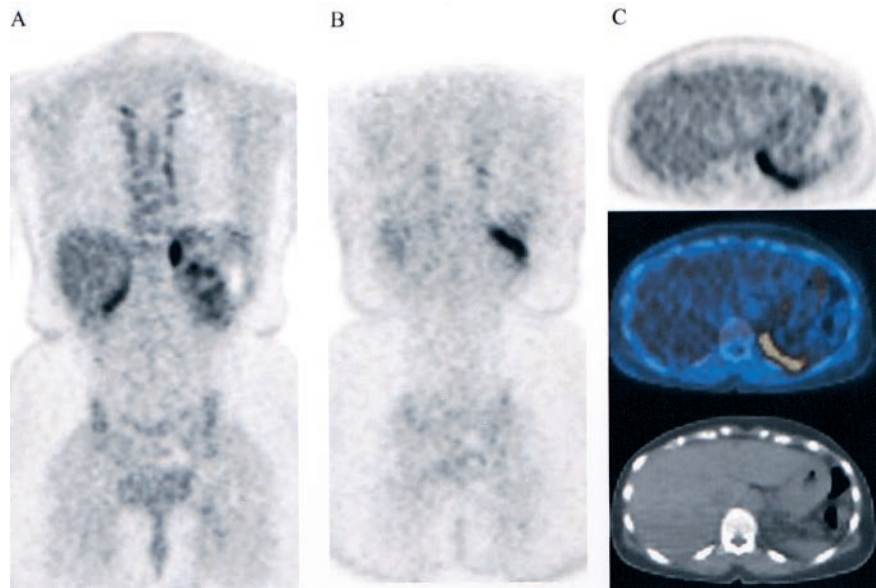
FIGURE 4. ^{18}F-FDG activity in perinephric fat may mimic adrenal (A) or rib (B) metastasis. (C) Transaxial slice of PET (top), CT (bottom), and fusion (middle) images localize ^{18}F-FDG activity to fat plane.

recent article, reported a similar SUV$_{max}$ (mean, 7.1; range, 2.08–17.35) in what they called "USA-Fat" (Uptake in Supraclavicular Area Fat) (7), confirming the frequently intense nature of ^{18}F-FDG uptake in adipose tissue.

Although the average SUV$_{max}$ for the group with muscle uptake was 5.8, the distribution of SUVs was skewed toward smaller values with a few notable lesions of very high uptake (Table 1). Specifically, in 9 of the 12 patients, the average was 3.8 (range, 3–5.8), comparable to the numbers

FIGURE 5. Transaxial slices of PET (A), CT (C), and fusion (B) images at upper chest level show ^{18}F-FDG activity mapped to adipose tissue among large vessels. ^{18}F-FDG activity is also seen in adipose tissue in supraclavicular regions bilaterally.

reported in Cohade's group (3.1 $\pm$ 1), suggesting that muscle uptake of ^{18}F-FDG is frequently low grade. The other 3 patients had intense ^{18}F-FDG uptake in individual neck muscles, with SUV$_{max}$ values of 10.9, 11.5, and 12.6, respectively. One of these patients had thoracic spine surgery shortly before the PET scan, which might cause abnormal muscle stress. No explanation could be found for the intense muscle uptake of ^{18}F-FDG in the other 2 patients.

An interesting observation was that neck fat occurred predominantly in females, whereas normal musculature was found more often in males (Table 2), the difference being statistically significant ($P < 0.01$, Fisher exact test). Neck fat was also seen significantly more in the younger age group. There were 26 pediatric patients ($\leq$17 y old) in the entire cohort, with 4 (15%) showing neck fat, in contrast to 837 adult patients, of whom 16 (1.9%) showed the same pattern ($P < 0.01$, Fisher exact test). Normal musculature, however, was seen only in adult patients.

In the group of patients showing neck fat, the mean body weight was 62.25 kg, and the mean BMI was 25.21. These numbers were not significantly different from that of the age- and sex-matched control group (64.18 kg and 25.94, respectively; $P = 0.37$ and 0.35, Wilcoxon test).

DISCUSSION

Curvilinear, usually fusiform-shaped ^{18}F-FDG uptake in the neck and shoulders has been observed in whole-body ^{18}F-FDG PET scans of occasional patients since the advent of body PET imaging in the mid 1990s. Because of the fusiform shape and the fact that it usually resolved, on repeat scanning, after pretreatment with diazepam, a muscle relaxant, it has always been accepted as muscle activity (1). So it came as a surprise when the PET/CT fusion images showed that sometimes the ^{18}F-FDG uptake was localized to
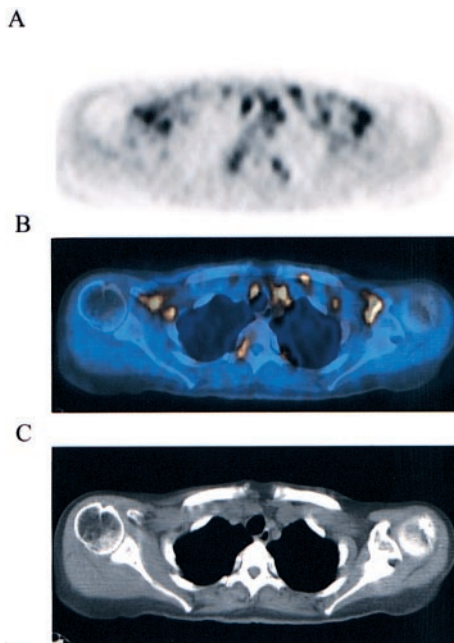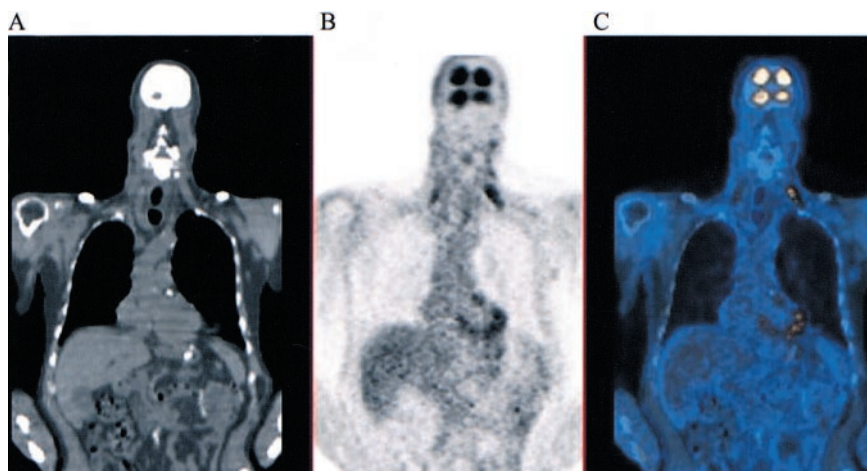
FIGURE 6. Coronal slices of CT (A), PET (B), and fusion (C) images show fusiform 18F-FDG activity mapped to scalenus muscle bilaterally. Patient has recent pharyngolaryngectomy for cancer, which may account for increased muscle activity.

TABLE 1
Details of All Patients Included in Study

Patient no.	Age (y)	Sex	Diagnosis	Patterns of 18F-FDG uptake (SUV$_{max}$)	Muscles visualized
1	43	F	Lung cancer	A, B	
2	12	F	Rhabdomyosarcoma	A (13.6), B (3.7), D (4.9)	
3	19	F	Osteosarcoma	A (7.1)	
4	59	F	Rectal cancer	A (10.2), B (5.9), D (7)	
5	8	M	Neuroblastoma	A (20), B (8.6), C (13)	
6	49	F	Gastric cancer	A (19), B (8.5), C (13.8), D (5.2)	
7	2	F	Rhabdomyosarcoma	A (3.3)	
8	24	M	Lymphoma	A (5.6), C (5.2)	
9	60	F	Colon cancer	A (4.2)	
10	35	F	Ovarian cancer	A (4.6), D (4.4)	
11	4	F	Neuroblastoma	A (1.9)	
12	34	F	Breast cancer	A (6.6), B (3.2)	
13	68	F	Lymphoma	A (3.8), B (4)	
14	56	F	Lung cancer	A (13.4), B (4.6), D (13.1)	
15	35	F	Ewing's sarcoma	A (5.4), B (4.1), C (5.1), D (4.4)	
16	56	F	Breast cancer	A (10), C (3.7)	
17	30	F	Hepatoma	A (6.1), B (3.4), C (4.7), D (4.4)	
18	67	F	Colon cancer	A (4.6)	
19	56	F	Lymphoma	A (3.8), B (2.8), D (4.5)	
20	25	M	Testicular cancer	A (2.8), B (2.5), C (3.2)	
21	44	F	Larynx cancer	E (10.9)	Erector spinae, infraspinatus
22	22	M	Neuroblastoma	E (12.6)	Levator scapulae
23	53	M	Lymphoma	E (5.8)	Longus collis, scalenus
24	56	M	Larynx cancer	E (3.5)	Trapezius
25	62	M	Nasopharyngeal cancer	E (3)	Scalenus anterior
26	50	M	Thyroid cancer	E (3.3)	Semispinalis capitis, oblique capitis
27	58	M	Larynx cancer	E (4)	Right scalenus
28	53	M	Head and neck cancer	E (3.9)	Scalenus
29	19	F	Hodgkin's disease	E (4.4)	Erector spinae, trapezius, semispinalis cervicis
30	50	M	Thyroid cancer	E (3.6)	Erector spinae, semispinalis cervicis, scalenus
31	69	F	Lung cancer	E (3)	Levator scapulae
32	71	M	Bladder cancer	E (11.5)	Sternomastoid

SUV$_{max}$ = maximum standardized uptake value.

Patterns of nonpathologic 18F-FDG uptake are neck fat (A), paravertebral uptake (B), perinephric fat (C), mediastinal fat (D), and normal musculature (E).

TABLE 2
Patient Characteristics of Different Patterns of Nonpathologic ^{18}F-FDG Uptake

Pattern	Neck fat	Paravertebral uptake*	Perinephric fat*	Mediastinal fat*	Normal musculature†
No. (%)	20 (2.3)	12 (1.4)	7 (0.8)	8 (0.9)	12 (1.4)
Sex (M/F)	3/17	2/10	3/4	0/8	9/3
Mean age‡ (y)	37 (2–68)	39 (8–68)	32 (8–56)	42 (30–59)	51 (19–71)
Mean SUV$_{max}$‡	7.7 (1.9–20)	4.7 (2.5–8.6)	7.0 (3.2–13.8)	6.0 (4.4–13.1)	5.8 (3–12.6)

*Always associated with neck fat, singly or in combination.
†Not associated with any other patterns.
‡Range in parentheses.

the adipose tissue rather than the muscle. In this study of 863 ^{18}F-FDG PET scans, we found ^{18}F-FDG uptake in the adipose tissue of the neck and supraclavicular region in 20 patients (2.3%). This is remarkably similar to the findings of Hany, who reported an incidence of 2.5% in 638 patients (6). Cohade et al., however, reported an incidence of 4% with the "USA-Fat" pattern in 347 patients (7). They also reported a higher incidence of increased ^{18}F-FDG activity in neck muscles (5.8% vs. 1.4% in this series). Part of this may be due to patient inclusion criteria. Although they selected patients with "faint uptake or greater," we included only patients with definitely increased ^{18}F-FDG activity.

Additionally, in about one third of this group of patients, we saw ^{18}F-FDG activity localized to the adipose tissue in the perinephric region and among the large vessels in the mediastinum. To our knowledge, this finding has not been reported in the literature. Because of the locations of the ^{18}F-FDG activity, this could easily be misinterpreted as adrenal metastases, lower rib metastases, or malignant lymph nodes in the mediastinum. In this situation, measurement of the SUV is not helpful in differentiating between malignant and benign etiology. As shown in this group of patients, ^{18}F-FDG activity in adipose tissue can be very intense, with the SUV$_{max}$ as high as 20 in 1 patient. Occasionally it can obscure real findings when a malignant lymph node is mixed in with the subcutaneous fat and assumed to be benign ^{18}F-FDG uptake in adipose tissue.

Paravertebral uptake describes the characteristic longitudinal array of ^{18}F-FDG foci along both sides of the thoracic spine, shown on the PET/CT images to be in the intercostal spaces. In the past, it has always been assumed to be due to muscle tension in anxious patients. Because of the complexity of the anatomy at this location, even with the fusion images, we cannot determine whether the ^{18}F-FDG activity localizes in the muscle, the costovertebral joints, or the adipose tissue. However, in this study all of the patients showing this pattern also showed neck fat, suggesting a common etiology—that is, uptake in adipose tissue.

In this series, ^{18}F-FDG activity was mapped to well-defined muscles in 12 patients (1.4%). In some patients, possible causes of abnormal muscle tone were present, such

as prior head and neck surgery or radiation therapy. The intensity of ^{18}F-FDG uptake in the muscles was low to moderate in the majority of patients (9/12), with the SUV$_{max}$ ranging from 3 to 5.8. In the other 3 patients, however, there was intense ^{18}F-FDG activity in individual muscles, with the SUV$_{max}$ >10. One of these patients had recent surgery in the vicinity that might have caused increased muscle tension. In the other 2 patients, the reason for the intense ^{18}F-FDG uptake remained unknown.

With PET/CT the true nature of the ^{18}F-FDG activity can usually be resolved on the fusion image. However, when the PET scan is obtained on a dedicated PET scanner without the benefit of the fusion images, it may be impossible to sort out the true nature of the increased ^{18}F-FDG activity. It is imperative that different patterns of ^{18}F-FDG uptake in adipose tissue be recognized and that the possibility of benign fat activity be considered whenever correlative imaging (CT or MRI) or the clinical picture is discordant with the PET findings. When in doubt, a repeat scan with PET/CT or after pretreatment with diazepam is usually helpful.

It is well known that fat cells contain the glucose transporter GLUT4, associated with insulin-mediated glucose uptake in adipose tissue (8–10). This may explain the visualization of ^{18}F-FDG activity in adipose tissue. Why we see it in only a small number of patients and in well-defined patterns is not well understood.

There are 2 types of adipose tissue in the human body: white adipose tissue (WAT) and brown adipose tissue (BAT). WAT provides insulation and serves as an energy depot. BAT, on the other hand, has the unique ability to generate heat in response to cold exposure (nonshivering thermogenesis) or ingestion of food (diet-induced thermogenesis), associated with increased glucose uptake (11). In contrast to WAT, BAT expresses mitochondrial uncoupling protein (UCP), which causes uncoupling of oxidative phosphorylation in the mitochondria and, hence, generation of heat directly rather than adenosine triphosphate (ATP). During this process, the metabolism of glucose via the anaerobic pathway is increased to provide the ATP that is necessary for fatty acid oxidation.

BAT is normally found in the neck, near large vessels in the chest, the axillae, the perinephric regions, the intercostal spaces along the spine, and the paraaortic regions (12,13), the locations where ^{18}F-FDG uptake in adipose tissue is seen in this study. This suggests that the ^{18}F-FDG accumulation is in BAT. The fact that there are small deposits of BAT along the spine also lends support to the assumption that the paravertebral ^{18}F-FDG uptake is BAT related.

BAT is most prominent in newborns and diminishes with age to virtually disappear in adults. Our observation that neck fat occurs more often in the younger age group is in agreement with this trend, although we see it in an age group older than expected. However, it has been shown that outdoor workers in Finland retained active BAT in adulthood, probably an adaptive change for cold-induced thermogenesis (14). It is possible that BAT persists into adulthood more often than was realized and can be stimulated by cold exposure, resulting in increased glucose metabolism in the process of thermogenesis.

BAT is rich in sympathetic nerves and adrenergic receptors, and glucose uptake by BAT is significantly increased by sympathetic nervous stimulation (15,16). This may explain the effectiveness of diazepam in abolishing the neck and shoulder ^{18}F-FDG uptake as reported previously (1). Peripheral-type benzodiazepine receptors have also been described on BAT of rats (17–20), suggesting a possible direct action of diazepam on the metabolism of BAT.

Recently, Okuyama et al. demonstrated that metaiodobenzylguanidine (^{123}I- or ^{125}I-MIBG) accumulated in BAT in rats (21) and suggested that the bilateral supraclavicular uptake sometimes seen on MIBG scans of patients without evidence of disease (22) was also due to tracer uptake in BAT. It is interesting to note that this normal variant on MIBG scan bears a striking resemblance to neck fat in our study, supporting the hypothesis that both MIBG and ^{18}F-FDG localize in BAT.

The BAT thermogenic response to cold has been found to be sex dependent in rodents (23). Rodriguez et al. showed that testosterone-treated cells showed a dose-dependent inhibition of mitochondrial uncoupling protein 1 (UCP1) messenger RNA expression under adrenergic stimulation by norepinephrine (24). Because UCP1 plays a central role in the thermogenesis in BAT, the effect of testosterone provides a molecular basis for our observation that neck fat is seen more in females. The same female predominance was also seen in the studies of Cohade et al., 12 females/2 males (7); Hany et al., 15 females/2 males (6); and Barrington and Maisey, 6 females/no males (1).

Some questions remain unanswered. We still do not know why this pattern occurs only in a small minority of patients. In a previous study, patients who had more extensive ^{18}F-FDG uptake in fat had a lower BMI than the other patients (6). However, our data show that the body weight and BMI of the group of patients showing ^{18}F-FDG uptake in adipose tissue are not statistically different from those of an age- and sex-matched control group. This is in concordance with the findings of Cohade et al., where the BMI of the group with ^{18}F-FDG uptake in fat was not significantly different from the groups with ^{18}F-FDG uptake in muscles and lymph nodes (7). Anxiety causing increased sympathetic nervous activity may cause increased glucose uptake by BAT, but this pattern is not seen in all anxious patients. Of the 2 known stimuli of BAT thermogenesis, ingestion of food is unlikely because all patients fast before the PET scan. Cold exposure is certainly a possibility and may explain the slight difference in incidence of adipose tissue ^{18}F-FDG activity in different series. However, more work needs to be done for confirmation. It may well be that some patients are genetically predisposed to BAT thermogenesis, as suggested by Himms-Hagen as an explanation of why some persons remain lean for years with no effort to control food intake (11). When presented with the right stimulus, these patients would then show the pattern of ^{18}F-FDG uptake in adipose tissue as described in this study.

This study was initiated by the observation that unexplained neck uptake of ^{18}F-FDG was frequently mapped to the adipose tissue; hence, the patient selection started with neck uptake. In this analysis, the incidence of ^{18}F-FDG uptake in sites other than the neck was restricted to the patient population with neck fat uptake, and the true incidence of ^{18}F-FDG uptake in other sites might be slightly higher. However, our impression, based on experience in the past 12 mo with 2 PET/CT scanners, is that isolated fat uptake of ^{18}F-FDG in other sites is exceedingly unusual.

CONCLUSION

Increased ^{18}F-FDG uptake can be seen in individual muscles in the neck, as well as the adipose tissue in the neck, supraclavicular regions, around the large vessels in the mediastinum, the axillae, the perinephric regions, and unspecified tissue in the intercostal spaces along the thoracic spine in 3.7% of patients undergoing ^{18}F-FDG PET scanning, constituting a potential source of false-positive PET imaging. ^{18}F-FDG uptake in adipose tissue is seen more commonly in the pediatric population and in females. Based on the pattern of uptake as well as the age and sex distribution, we postulate that the ^{18}F-FDG activity in fat is localized in the BAT.

REFERENCES

1. Barrington S, Maisey M. Skeletal muscle uptake of fluorine-18-FDG: effect of oral diazepam. *J Nucl Med.* 1996;37:1127–1129.
2. Engel H, Steinert H, Buck A, Berthold T, Huch Boni R, von Schulthess G. Whole-body PET: physiological and artifactual fluorodeoxyglucose accumulations. *J Nucl Med.* 1996;37:441–446.
3. Hany T, Steinert H, Goerres G, Buck A, von Schulthess G. PET diagnostic accuracy: improvement with in-line PET-CT system: initial results. *Radiology.* 2002;225:575–581.
4. Kluetz P, Meltzer C, Villemagne V, et al. Combined PET/CT imaging in oncology: impact on patient management. *Clin Positron Imaging.* 2000;3:223–230.
5. Steinert H, Hany T, Kamel E, Lardinois D, Weber W, von Schulthess G. Impact

of integrated PETCT scanning on preoperative staging of lung cancer [abstract]. *J Nucl Med.* 2002;43(suppl):151P.

6. Hany T, Gharehpapagh E, Kamel E, Buck A, Himms-Hagen J, von Schulthess G. Brown adipose tissue: a factor to consider in symmetrical tracer uptake in the neck and upper chest region. *Eur J Nucl Med Mol Imaging.* 2002;29:1393–1398.

7. Cohade C, Osman M, Pannu HK, Wahl RL. Uptake in supraclavicular area fat ("USA-Fat"): description on ^{18}F-FDG PET/CT. *J Nucl Med.* 2003;44:170–176.

8. Ploug T, Ralston E. Exploring the whereabouts of GLUT4 in skeletal muscle. *Mol Membr Biol.* 2002;19:39–49.

9. Konrad D, Bilan P, Nawaz Z, et al. Need for GLUT4 activation to reach maximum effect of insulin-mediated glucose uptake in brown adipocytes isolated from GLUT4myc-expressing mice. *Diabetes.* 2002;51:2719–2726.

10. Kawashita N, Brito M, Brito S, et al. Glucose uptake, glucose transporter GLUT4, and glycolytic enzymes in brown adipose tissue from rats adapted to a high protein diet. *Metabolism.* 2002;51:1501–1505.

11. Himms-Hagen J. Thermogenesis in brown adipose tissue as an energy buffer. *N Eng J Med.* 1984;311:1549–1558.

12. Dawkins M, Hull D. The production of heat by fat. *Sci Am.* 1965;213:62–67.

13. Johansson B. Brown fat: a review. *Metabolism.* 1959;8:221–240.

14. Huttunen P, Hirvonen J, Kinnula V. The occurrence of brown adipose tissue in outdoor workers. *Eur J Appl Physiol Occup Physiol.* 1981;46:339–345.

15. Girardier L, Seydoux J. Neural control of brown adipose tissue. In: Trayburn P, Nicholls D, eds. *Brown Adipose Tissue*. London, U.K.: Edward Arnold; 1986: 123–147.

16. Hull D, Segall M. Sympathetic nervous control of brown adipose tissue and heat production in the new-born rabbit. *J Physiol.* 1965;181:458–467.

17. Anholt R, De Souza E, Oster-Granite M, Snyder S. Peripheral-type benzodiazepine receptors: autoradiographic localization in whole-body sections of neonatal rats. *J Pharmacol Exp Ther.* 1985;233:517–526.

18. Hirsch J. Pharmacological and physiological properties of benzodiazepine binding sites in rodent brown adipose tissue. *Comp Biochem Physiol C.* 1984;77: 339–343.

19. Parola A, Yamamura H, Laird H 3rd. Peripheral-type benzodiazepine receptors. *Life Sci.* 1993;52:1329–1342.

20. Zisterer D, Williams D. Peripheral-type benzodiazepine receptors. *Gen Pharmacol.* 1997;29:305–314.

21. Okuyama C, Sakane N, Yoshida T, et al. [123]I- or ^{125}I-metaiodobenzylguanidine visualization of brown adipose tissue. *J Nucl Med.* 2002;43:1234–1240.

22. Lumbroso J, Giammarile F, Hartmann O, Bonnin F, Parmentier C. Upper clavicular and cardiac meta-[^{123}I]iodobenzylguanidine uptake in children. *Q J Nucl Med.* 1995;39:17–20.

23. Rodriguez-Cuenca S, Pujol E, Justo R, et al. Sex-dependent thermogenesis, differences in mitochondrial morphology and function, and adrenergic response in brown adipose tissue. *J Biol Chem.* 2002;277:42958–42963.

24. Rodriguez A, Monjo M, Roca P, Palou A. Opposite actions of testosterone and progesterone on UCP1 mRNA expression in cultured brown adipocytes. *Cell Mol Life Sci.* 2002;59:1714–1723.